Fabrication and Results of the First MgB_2 Round Coil Superferric Magnet at LASA

S. Mariotto, A. Leone, A. Paccalini, A. Pasini, D. Pedrini, M. Prioli
M. Quadrio, M.Sorbi, M. Statera, M. Todero, R. Valente

***Abstract*— The LASA Laboratory (INFN, Milan) is working in the High Luminosity LHC program to develop, in collaboration with CERN, six different types of High Order corrector magnets. In this framework, in parallel with a conventional design of superferric magnets with LTS conductor, the LASA is focusing on the research of new superconducting materials which may have applications in particle accelerator magnets. To this purpose, LASA is developing a new type of superferric magnet suitable to arbitrary multipole order, called Round Coil Superferric Magnets (RCSM). The iron yoke shaped with an arbitrary number of poles is able to create the desired harmonic component using only one single round coil with a large bending radius suitable for very strain-sensitive superconductors. The electromagnetic design of a sextupole configuration of the magnet and the production of the first superconducting MgB2 round coil prototype have been already presented. In this paper, we expose the optimization of the iron yoke and polar expansions assembly of the first magnet semi-module prototype. The results of the whole powering test are described in detail and the analysis of the magnetic performances are compared with those of classical superferric correctors.**

***Index Terms* — Accelerator magnets: dipoles, quadrupoles, correctors, Quench Protection, Magnet design and analysis techniques, Magnesium boride wire, Superconducting Magnets**

I. INTRODUCTION

THE technological development of superconducting materials is considered having a key role in the construction of next-generation particle accelerator magnets. Different materials like HTS superconductors are currently used for windings and coils for magnet prototypes. In the collaboration framework between CERN and INFN-LASA (the Laboratory of Accelerators and Applied Superconductivity in Milan), six different High Order (HO) corrector magnets have been designed and are being built for the multiple corrector magnets string of the HL-LHC interaction region [1][2], which aims to increase the luminosity of the colliding beams by a factor of five more than the actual nominal value. The experience acquired for the construction of these prototypes, whose details can be found in [3]-[9], brought the LASA laboratories to the development of a new type of superferric corrector magnet suitable to superconducting strain sensitive materials which can produce an arbitrary multipole magnetic field order with simply round coils with large bending radius. The first idea of this particular design has been studied by I. F. Malyshev and V. Kashikhin [10] and optimized by G. Volpini and J. Rhysti who first tried to use MgB_2 tapes for the coil construction [11]. The optimization process of using MgB_2 wires instead of tapes in order to decrease the coil peak field and properly modify the iron poles saturation is reported in [12]. The RCSM (Round Coil Superferric Magnet) can be assembled in a modular configuration simplifying the construction process in which the semi-module prototype, built in a sextupole configuration, implements one single round coil made of MgB_2 winding. The modular lattice includes two round coils wound in opposite directions in order to erase the solenoidal contribution and enhance the sextupole field in the bore area. Firstly, one superconducting coil, whose details are reported in [13], and then the first semi-module configuration have been successfully tested in LASA laboratories, reaching the designed operational point without any training. Quench study simulations reproduced very well the performances of the single-coil test, in which the round coil has been powered without the iron yoke and poles, and their details have been used to perform the simulation for the semi-

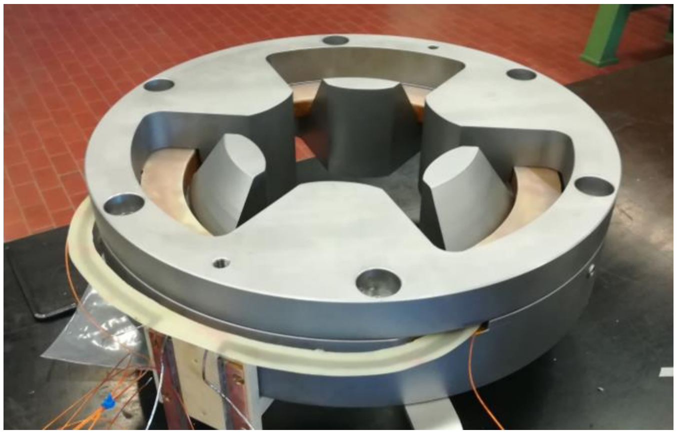

Fig. 1. First RCSM sextupole prototype successfully assembled and tested at LASA laboratories. The six poles confine the superconducting coil in the middle plane of the magnet. The coil ends are clearly visible outside the small aperture in the external side of the iron yoke and are soldered at the PCB layer for mechanical and electromagnetic stability.

S. Mariotto and M. Sorbi are with the Laboratory of Accelerators and Applied Superconductivity, National Institute for Nuclear Physics, MilanSection, Segrate 20090, Italy and also with the Department of Physics, University of Study of Milan, Milan 20122, Italy (e-mail: samuele.mariotto@mi.infn.it).

R. Valente is with Laboratory of Accelerators ans Applied Superconductivity, National Institute for Nuclear Physics, MilanSection, Segrate 20090, Italy and also with La Sapienza, University of Rome.

A. Leone, A. Paccalini, A. Pasini, D. Pedrini, M. Prioli, M. Quadrio, M. Statera and M. Todero are with the Laboratory of Accelerators and Applied Superconductivity, National Institute for Nuclear Physics, Milan Section, Segrate 20090, Italy.

module prototype test. In this paper, we present a brief summary of the magnet design, the construction process and prototype qualification, the quench studies and finally the test results. A second semi-module is foreseen to be built and tested in the modular configuration in the next couple of years. Magnetic field quality measurements, performed with the same rotating shaft used for the HO corrector prototypes [14], will be done in order to complete the characterization of the magnet.

II. MAGNET DESIGN

The sextupole configuration has a bore aperture diameter of 150 mm as in the classic superferric corrector one. The external ARMCO iron yoke diameter is equal to 400 mm and the length of the semi-module to 96 mm. The final magnet configuration, composed by two modules (4 round coils), has been designed to reach 67 T·mm of integrated main field at reference radius of 50 mm and at I_{nom} = 148.81 A. It is also required to be stable at the ultimate current I_{ult} = 161 A as an additional safety margin. Simulated semi-module load line and stand-alone coil one are reported in Fig. 2 and compared to the critical surface of the MgB_2 wire calculated at 4.2 K in order to fix the margin to 40% for the operational point of the two modules configuration magnet. Each pole is machined in the central region creating the slot for the superconducting coil with an internal diameter of 266 mm. The same bending diameter has been used during all the winding process of the coil in order not to degrade the conductor properties.

TABLE I
DESIGN FEATURES FOR RCSM PROTOTYPE

Operating Current	148.81	A
Ultimate Current	161	A
Magnet Short Sample Limit @ 4.2 K	333	A
Coil Short Sample Limit @ 4.2 K	300	A
Stored Energy @ I_{op}	1.1	kJ
Stored Energy @ I_{ult}	1.23	kJ
Low current Inductance	375	mH
Differential Inductance @ I_{op}	73	mH

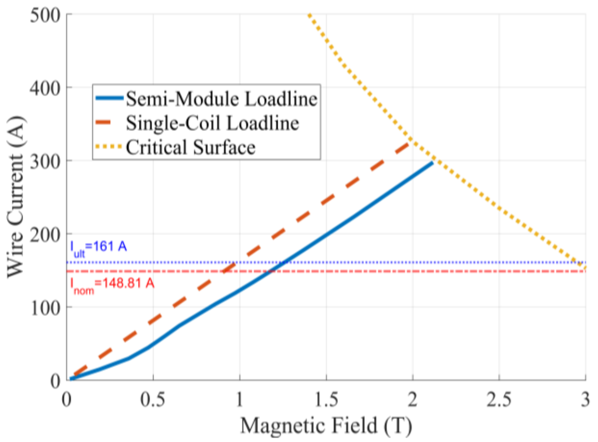

Fig. 2. RCSM semi-module loadline versus the critical surface calculated at 4.2 K. The horizontal dot and dash-dot lines are the I_{nom} and I_{ult} of the final magnet (2 modules).

TABLE II
MgB_2 WIRE COMPOSITION

MgB	Monel	Niobium	Nickel	Copper
11.5%	46%	14.5%	14%	14%

The wire, produced by Columbus Industry in Genoa, is a single strand with a non-insulated diameter of 1 mm. Due to machining problems in the insulation process, the wire has been covered with polyester instead of S-2 Glass. The strand is composed of 37 filaments of 55 μm diameter surrounded by a niobium barrier and embedded in a Monel matrix. Wire composition can be found in Table II. Material fractions of the wire have been averaged as simulated properties of the coil elementary cell for the quench propagation analysis. The round coil is composed of 336 turns placed in 28 layers and ground insulated with one 1.2 mm thick layer of BTS-2 in the axial direction and 0.15 mm thick in the radial one. The coil cross-section is 32.3 mm in the radial direction and 18 mm in the axial one. The coil ends are connected to the external power supply through MgB_2-NbTi soldering on a PCB layer which exits from the iron yoke through two apertures in the semi-module middle plane. This layer creates mechanical and electromagnetic stability of the coil leads, which are then soldered to copper plates for bus bar connection to avoid stresses on the wire. Mechanical containment of the coil is performed by 6 spring washers, placed radially in the middle of each pole and preloaded before cooldown. Axial preload of the iron yoke is applied by Cu-Be rods whose length can be adjusted for different modular configuration of the magnet.

III. PROTOTYPE ASSEMBLY

The particular shape of iron poles in the RCSM prototype cannot be easily reproduced using iron laminations. Therefore, firstly an electrical discharge machine and, secondly, a CNC machine have been used to control poles surface uniformity and quality. Two cylinders of ARMCO Iron have been machined in order to obtain two symmetrical halves of the semi-module, thus allowing the insertion of the MgB_2 coil. Axial alignment of the two halves is assured by creating a small groove at the outer radius, while rotational alignment is produced by one key Cu-Be rod. Coil ends have been insulated from ground by adding a layer of polyimide on iron slots walls and its centering alignment has been performed by adding spacers in the internal gap between the coil and iron poles. A 0.15 mm thick layer of Teflon has been inserted between the coil upper face and the 3 downwards iron poles to allow their relative displacements during magnet cool down or powering. Packs of spring washers have been preloaded to 730 N each one in order to avoid coil detachment during cool down and assure the existence of an equilibrium position while powering. This mechanical system has been tested and validated during the single-coil powering test with the spring washers mounted on an aluminum plate because of the lack of the iron yoke. Electrical Insulation tests have been done before cooldown to verify ground insulation of the tested coil.

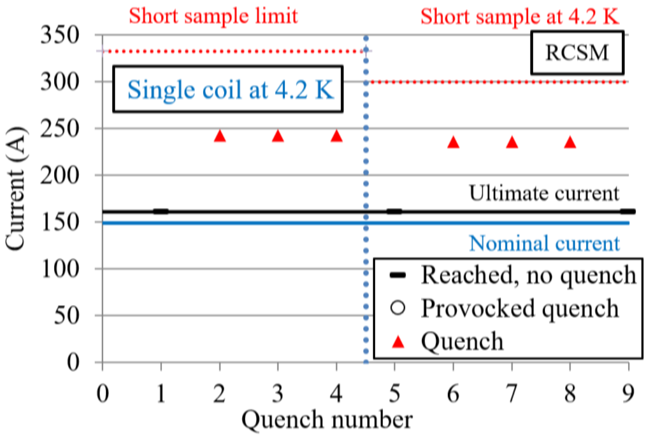

Fig. 3. Summary of the RCSM semi-module prototype powering test performed at INFN LASA compared to the single coil test done in March 2018.

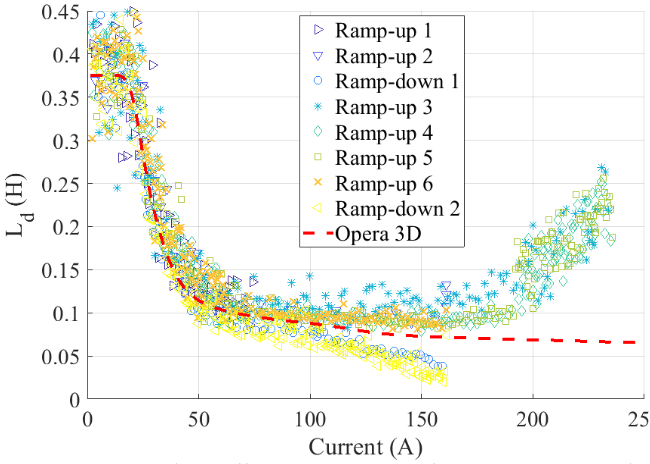

Fig. 4. Analysis of the differential inductance of the semi-module configuration compared to values in red dashed line retrieved by OPERA 3D simulations. Dots colors are linked to the different ramp up or ramp down performed during the cryogenic test.

IV. POWERING TEST

The semi-module prototype powering test has been performed at LASA laboratories at 4.2 K in a vertical cryostat. Cooldown has been monitored by means of two CGR-500 temperature probes mounted on the upper and lower faces of the magnet. Temperature ramp-down has been controlled to be under 40 K/h and to have a temperature gradient below 100 K/m. The main goal of the test was to demonstrate the safety of the coil up to the same level of mechanical stress and load line working point of the final magnet achieving the ultimate current and performing a 1-hour stability test according to the standards required for the HO Corrector magnets for HL-LHC. Test results are summarized in Fig. 3 and compared to single coil test performances. The prototype did not show training, reaching the ultimate current and being stable for the 1-hour test. Higher values of current have been explored in the test in order to study the prototype performances and evaluate the degradation of the superconducting coil. A ramp rate of 0.2 A/s has been used at low values of current and a maximum of 0.5 A/s ramp rate at high values. Three consecutive quenches occurred at 236 A, like in the single-coil test (which happened at 234 A and 73% of the load line), limiting the semi-module performance to 78% of the load line. This limit is compatible with the previously measured degradation, see [13] for further details, of the samples taken from the winding ends showing that the coil connections with the PCB represent the most critical step for the construction process. A second 1-hour stability test has been performed at the end of the test to confirm the magnet integrity. Even if the external insulation layer of the coil during the single-coil test showed cracks, no additional visible coil damage or deformations have been noticed after prototype test.

A. *Quench Study*

The protection study has been executed with QLASA code [15] and LTSpice which run in a co-simulation in the STEAM environment [16]. The QLASA code simulates the quench propagation inside the coil using the material properties taken from the MATPRO database, while LTSpice calculates the current variation in the equivalent circuit of the powering system, due to the rise of the coil resistance, and change the inductance of the magnet equivalent inductor as a function of current. Electromagnetic features of the prototype like inductance of the coil and magnetic field map have been reproduced in finite element OPERA 3D simulations [17]. In particular, the magnet differential inductance has been calculated using electromagnetic static solver and compared to experimental results obtained from the magnet dividing the total voltage by the current ramp rate. Different ramps up and down have been analyzed during the test. As we can see in Fig. 4, small differences in differential inductance have been observed during different ramps of the magnet. In particular, the two ramps down from ultimate current to null value describe a differential inductance lower than the simulated value, while all the other ramps up seem to have higher values than the simulated one. Specifically, above the value of 200 A of current, an increasing differential inductance has been retrieved from measurements. This same behavior has been observed in the analysis of the single-coil powering test. In the single-coil test, the differential inductance is compatible with a constant value of 55.9 mH, as simulated with OPERA 3D, for values of operational current below of 200 A and increase with higher values. The main hypothesis under study is the smooth transition to the normal conductive state of the winding ends which represents the weak spot of the entire coil. This positive resistive contribution to coil voltage cannot be separated from the negative inductive signal, because of lack of internal voltage taps, therefore resulting in a higher equivalent differential inductance value. The quench protection scheme adopted for the semi-module magnet is the same used for the single-coil powering test. Only the coil ends are connected to the detection system and no internal voltage taps are installed. A total voltage threshold of 100 mV and a validation time of 20 ms have been chosen for the quench detection system. A dumping resistance of 1 Ohm is used to extract the coil energy during the quench propagation. Coil connections to the copper plates, stabilized by the use of the Nb-Ti wire with which they are soldered on the PCB, are monitored in the quench protection scheme in order to verify the starting point of the quench inside the magnet. After the first quench occurred at 236 A, the voltage threshold has been changed to 150 mV to evaluate the changes in magnet resistance development and the operating margin for the protection scheme. In Fig. 5 and Fig. 6 we report the current decay and the voltage drop measured during the last quench at 236 A and compare them with simulations. The experimental discharge of the magnet is faster than the simulated one, suggesting that eddy currents in the non-laminated iron or in the superconductor are created during the fast decay. This behavior has been already seen for the single-coil test where eddy currents in the aluminum supporting plate had been included to better describe the current decay. Simulations of the eddy currents in the non-laminated iron are currently in progress analyzing their variability as a function of the iron magnetization and coil instantaneous current.

B. *Transfer Function*

The magnetic field produced by the prototype has been measured using a Hall probe. A G10 frame has been used to fix the probe position at the reference radius, equal to 50±1 mm, in front of a pole, and longitudinally centered with the magnet in the axial direction. Calibration of the hall probe has been validated during tests of HO Corrector prototypes and no drifts of the signal among different cooldowns have been seen. RCSM test results reported in Fig. 4 show high repeatability of the measurements during different ramps of the magnet assuring no degradation of the coil. If compared to simulations, the measurements can be reproduced within 7% of error. The main source of error in the measurements comes from the radial and axial positioning of the Hall probe which has to be very accurate ($\leq \pm 1$ mm) in order to deal with the strongly changing magnetic field: the difference with measurements decreases to 4.5% if a 1 mm radial displacement is considered. However, we have also to consider a possible error coming from the uncertainty of the BH curve, taken from HL-LHC iron specifications, which can be different from the one of the ARMCO Iron used for the magnet. As expected and observed in the simulations, at high values of current above 120 A, the rotation of the magnetic field towards the axial direction of the magnet is clearly visible. In fact, while the coil contribution, along the rotational axis of the magnet, continues to grow, the radial contribution, due to the iron poles, saturates. Increasing the current, the magnetization of the iron poles is induced to enhance the solenoidal field of the coil rather than the radial desired harmonic component inside the magnet bore.

V. CONCLUSION

The First RCSM prototype, in the Sextupole semi-module configuration, has been constructed and successfully tested. The magnet reached, firstly, the nominal current and, secondly, the ultimate one without any quench. The maximum current reached is equal to 236 A (78% of S.S.L. @ 4.2 K) which is compatible with wire degradation seen during the single-coil test and that is reasonably due to the winding process. Further analysis of the magnetic field produced has to be done in order to verify the magnet efficiency. Quench analysis showed that experimental decay is faster than the simulated one. Different hypotheses are still under discussion but the results of the RCSM prototype test are encouraging and they open to the construction of the whole modular operating magnet.

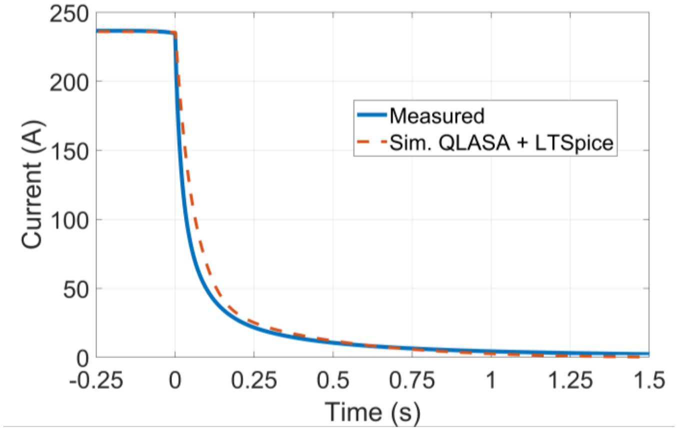

Fig. 5. RCSM current decay during the last quench occurred at 236 A. The measured signal is compared with the simulation obtained by the STEAM co-simulation between LTSpice and QLASA.

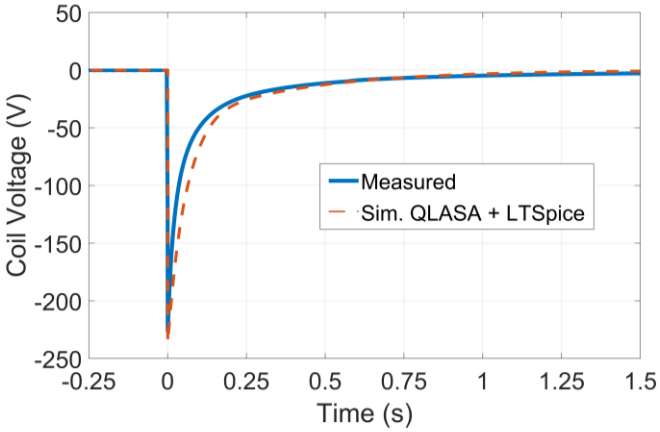

Fig. 6. RCSM total voltage across the ends of the coil during the last quench occurred at 236 A. The measured signal is compared with the simulation obtained by the STEAM co-simulation between LTSpice and QLASA.

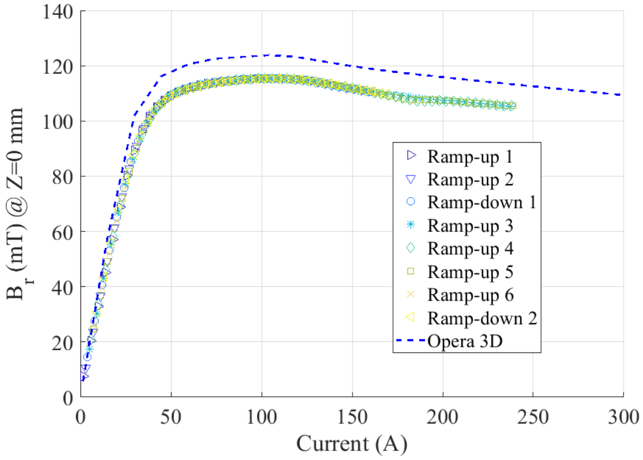

Fig. 7. Hall probe signal measured with a 1 Hz rate during all the magnet test. The different ramps of the magnet are shown and compared to the radial magnetic field calculated with Opera 3D simulations. Each ramp is performed with ramp rates from 0.2 A/s to a maximum of 0.5 A/s.

REFERENCES

[1] E. Todesco, H. Allain, G. Ambrosio, G. Arduini, F. Cerutti, R. D. Maria, L. Esposito, S. Fartoukh, P. Ferracin, H. Felice, R. Gupta, R. Kersevan, N. Mokhov, T. Nakamoto, I. Rakno, J. M. Rifflet, L. Rossi, G. L. Sabbi, M. Segreti, F. Toral, Q. Xu, P. Wanderer, and R. van Weelderen, “A First Baseline for the Magnets in the High Luminosity LHC Insertion Regions” IEEE Transactions on Applied Superconductivity, vol. 24, pp. 1–5, June 2014.

[2] G. Volpini, F. Alessandria, G. Bellomo, F. Broggi, A. Paccalini, D. Pedrini, A. Leone, M. Quadrio, L. Somaschini, M. Sorbi, M. Todero, C. Uva, P. Fessia, E. Todesco, and F. Toral, “NbTi Superferric Corrector Magnets for the LHC Luminosity Upgrade” IEEE Transactions on Applied Superconductivity, vol. 25, pp. 1–5, June 2015.

[3] M. Sorbi, F. Alessandria, G. Bellomo, F. Broggi, A. Leone, V. Marinozzi, S. Mariotto, A. Musso, A. Paccalini, D. Pedrini, M. Quadrio, M. Statera, M. Todero, E. Todesco, and C. Uva, “Status of the Activity for the Construction of the HL-LHC Superconducting High Order Corrector Magnets at LASA-Milan” IEEE Transactions on Applied Superconductivity, vol. 28, pp. 1–5, April 2018.

[4] G. Volpini, F. Alessandria, G. Bellomo, F. Broggi, A. Paccalini, D. Pedrini, A. Leone, V. Marinozzi, M. Quadrio, M. Sorbi, M. Statera, M. Todero, C. Uva, P. Fessia, A. Musso, E. Todesco, and F. Toral, “Development of the Superferric Sextupole Corrector Magnet for the LHC Luminosity Upgrade” IEEE Transactions on Applied Superconductivity, vol. 26, pp. 1–4, June 2016.

[5] M. Statera, G. Volpini, F. Alessandria, G. Bellomo, F. Broggi, A. Paccalini, D. Pedrini, A. Leone, V. Marinozzi, M. Quadrio, M. Sorbi, M. Todero, C. Uva, P. Fessia, A. Musso, E. Todesco, and F. Toral, “Construction and Cold Test of the First Superferric Corrector Magnet for the LHC Luminosity Upgrade” IEEE Transactions on Applied Superconductivity, vol. 27, pp. 1–5, June 2017.

[6] M. Statera, F. Alessandria, F. Broggi, A. Leone, V. Marinozzi, S. Mariotto, A. Paccalini, D. Pedrini, M. Quadrio, M. Sorbi, M. Todero, C. Uva, P. Fessia, A. Musso, and E. Todesco, “Construction and Cold Test of the Superferric Octupole for the LHC Luminosity Upgrade” IEEE Transactions on Applied Superconductivity, vol. 28, pp. 1–5, June 2018.

[7] M. Statera *et al*, “Construction and Cold Test of the Superferric Decapole for the LHC Luminosity Upgrade” IEEE Transactions on Applied Superconductivity, vol. 29, no. 5, pp. 1–5, 2019.

[8] M. Sorbi *et al*, “Construction and Cold Test of the Superferric Dodecapole High Order Corrector for the LHC High Luminosity Upgrade” IEEE Transactions on Applied Superconductivity, vol. 29, no. 5, pp. 1–5, 2019.

[9] M. Statera *et al*, “Construction and Cold Test of the Superferric Skew Quadrupole for HL-LHC” IEEE Transactions on Applied Superconductivity, vol. 30, no. 4, June 2020.

[10] V. Kashikhin, “A Novel Design of Iron Dominated Superconducting Multipole Magnets with Circular Coils” IEEE Transactions on Applied Superconductivity, vol. 20, pp. 196–199, June 2010.

[11] G. Volpini, J. Rysti, and M. Statera, “Electromagnetic Study of a Round coil Superferric Magnet” IEEE Transactions on Applied Superconductivity, vol. 26, pp. 1–5, June 2016.

[12] S. Mariotto, V. Marinozzi, J. Rysti, M. Sorbi, and M. Statera, “Study of a Sextupole Round Coil Superferric Magnet” IEEE Transactions on Applied Superconductivity, vol. 28, pp. 1–5, April 2018.

[13] S. Mariotto *et al*, "Activity on the Sextupole Round Coil Superferric Magnet Prototype at LASA" IEEE Transactions on Applied Superconductivity, vol. 29, no. 5, pp. 1-5, Aug. 2019, Art no. 4004505.

[14] L. Fiscarelli, H. Bajas, F. Mangiarotti, A. Musso, S. Russenchuck, S. Mariotto, M. Sorbi, and M. Statera, “Magnetic Measurements on the Prototype Magnets of the High-Order Correctors for HL-LHC” IEEE Transactions on Applied Superconductivity, vol. 29, pp. 1–5, Aug 2019.

[15] L. Rossi and M. Sorbi, “QLASA: a computer code for quench simulation in adiabatic multi-coil superconducting windings” Tech. Rep. TC-04-13, INFN - Milano, 2004.

[16] STEAM: Simulation of Transient Effects in Accelerator Magnets, https://espace.cern.ch/steam/

[17] COBHAM, OPERA-3D, “Vector field software” Cobham Technical Services, Vector Fields Software, UK, 1999-2013. Available at https://operafea.com/